NANO LETTERS

pubs.acs.org/NanoLett

Letter

Excitonic Fine Structure in Emission of Linear Carbon Chains

Stella Kutrovskaya,* Anton Osipov, Stepan Baryshev, Anton Zasedatelev, Vladislav Samyshkin, Sevak Demirchyan, Olivia Pulci, Davide Grassano, Lorenzo Gontrani, Richard Rudolph Hartmann, Mikhail E. Portnoi, Alexey Kucherik, Pavlos G. Lagoudakis, and Alexey Kavokin

Cite This: *Nano Lett.* 2020, 20, 6502–6509

Read Online

ACCESS | Metrics & More | Article Recommendations | Supporting Information

ABSTRACT: We studied monatomic linear carbon chains stabilized by gold nanoparticles attached to their ends and deposited on a solid substrate. We observe spectral features of straight chains containing from 8 to 24 atoms. Low-temperature PL spectra reveal characteristic triplet fine structures that repeat themselves for carbon chains of different lengths. The triplet is invariably composed of a sharp intense peak accompanied by two broader satellites situated 15 and 40 meV below the main peak. We interpret these resonances as an edge-state neutral exciton and positively and negatively charged trions, respectively. The time-resolved PL shows that the radiative lifetime of the observed quasiparticles is about 1 ns, and it increases with the increase of the length of the chain. At high temperatures a nonradiative exciton decay channel appears due to the thermal hopping of carriers between parallel carbon chains. Excitons in carbon chains possess large oscillator strengths and extremely low inhomogeneous broadenings.

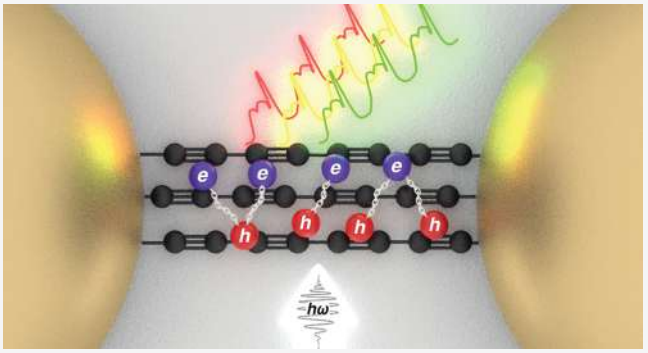

KEYWORDS: *carbon chains, excitons, photoluminescence spectra, nanoparticles*

Several types of low-dimensional crystals based on carbon were attracting the attention of the physical and chemical research communities in the XXI century. Nanodiamonds, fullerenes, carbon nanotubes, and graphene demonstrate a variety of interesting and unusual electronic properties that make them promising for a variety of applications in nanoelectronics and photonics.[1] One of the most challenging goals for the nanofabrication technology is the realization of ultimate one-dimensional crystals, monatomic chains of sp-carbon. Traces of two stable allotropes of sp-carbon (polyyne and cumulene) have been found in nature: in meteorite craters, interstellar dust, natural graphite, and diamond mines.[2−6] The high chemical reactivity of linear acetylenic carbon and its low stability at room temperature and atmospheric pressure make it difficult to extract freestanding carbon chains from natural sources. Moreover, multiple attempts to synthesize polyyne chains artificially have yielded modest or no success so far.[7] Until now, to the best of our knowledge, stable freestanding samples of straight carbon chains have not yet been realized. Their synthesis appears to be a formidable challenge as, in general, infinite one-dimensional atomic chains are unstable in vacuum. According to the Landau theorem,[8] fluctuations prevent the formation of ideal one-dimensional crystals. Therefore, many works have been devoted to the artificial stabilization of carbon chains. The stabilization may be achieved by the use of heavy anchor atomic groups.[9] The fabrication of carbon chains with *in situ* TEM allowed the production of chains of about 5 nm in length.[10] The synthesis of carbon chains inside double-wall nanotubes[11] was shown to be an efficient way for the realization of macroscopically long carbon isolated from the environment. In order to fabricate freestanding chains, the pinning to metal surfaces has been used.[12] The stabilization of carbon chains by the tris(3,5-di-*t*-butylphenyl)methyl moiety led to the observation of a record 44 atom long freestanding chain.[13] One-dimensional carbon crystals are expected to exhibit unique mechanical, optical, and electronic properties.[14] According to the recent theoretical works,[15] one-dimensional carbon chains could form the most robust of all known crystals. It may take one of two allotropic forms: cumulene, where neighboring carbon atoms are linked with double electronic bonds, and polyyne, where single and triple electronic bonds alternate (see the schematic in see Figure 1a.). Note that here we mean by polyyne a series of consecutive alkynes, $(—C{\equiv}C—)_n$ with n greater than 1 and is not necessarily ended by hydrogen atoms. In polyyne, the interatomic distances are predicted to be 0.133 nm (C—C)

Received: May 28, 2020
Revised: July 29, 2020
Published: July 30, 2020

https://dx.doi.org/10.1021/acs.nanolett.0c02244
Nano Lett. 2020, 20, 6502–6509

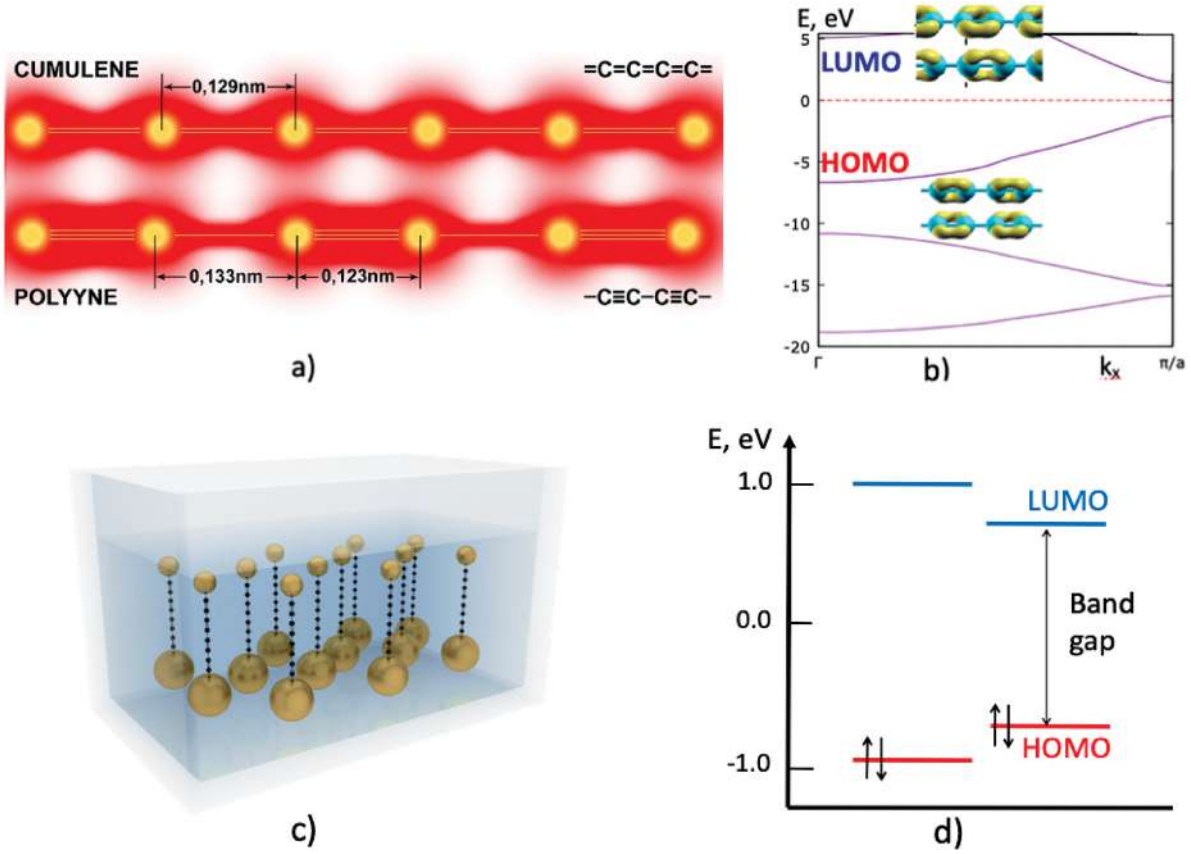

Figure 1. Structure of monatomic carbon chains: (a) Schematic distribution of the electron density in cumulene and polyyne allotropes. (b) Band structure of an infinite polyyne chain predicted by our *ab initio* calculation, and the HOMO, LUMO doubly degenerate orbitals. (c) Concept of stabilization of monatomic carbon chains by gold nanoparticles (NPs) in a solution. Gold NPs are shown out of the actual scale. (d) Energy level structure of a finite polyyne chain composed by 14 carbon atoms with two gold nanoparticles attached to its ends.

and 0.123 nm (C≡C) which yields the lattice constant of 0.256 nm. These interatomic separations are significantly less than those in graphite where the spacing between neighboring atoms is 0.142 nm, while the spacing between atomic planes is 0.335 nm. This is why the predicted Young's modulus of linear carbon chains is somewhat higher than in graphene and 1 order of magnitude higher than that of diamond.[16] *Ab initio* calculations[15] show that infinite-chain polyyne is a direct band gap semiconductor, with a gap of 2.58 eV. Our own *ab initio* calculations of the band structure of stabilized infinite polyyne chains predict the existence of a direct electronic band gap of 2.7 eV at the edge of the Brillouin zone (see Figure 1b). Being direct-gap semiconductors, polyyne chains are expected to possess unusual optical properties. In particular, their nonlinear optical response is expected to be giant.[17] Indeed, unlike graphite or graphene which are strong absorbers and do not emit light and carbon nanotubes where the multivalley band structure leads to dark excitons suppressing the luminescence, one-dimensional carbon crystals are attractive because of their ability to emit visible light. Room temperature photoluminescence (PL) spectra of carbon chains previously reported[18] demonstrate a sequence of broad maxima corresponding to the chains of different lengths. The band gap of finite size linear chains dramatically depends on the number of carbon atoms in a chain, getting larger in shorter chains. In the following we shall focus on straight polyyne chains containing from 8 to 24 carbon atoms whose band structure is reduced to a sequence of discrete energy levels similar to molecular orbitals. The gap between the highest occupied molecular orbital (HOMO) and the lowest unoccupied molecular orbital (LUMO) varies in the range 2−4 eV (see the schematic in Figure 1d). This results in a large spectral distribution of allowed optical transitions in such systems.

In this Letter, we study stable polyyne chains synthesized by the laser ablation (LAL) technique in a colloidal solution. The mechanical stabilization of sp-carbon is achieved due to the electron bonding of carbon chains to gold nanoparticles (NPs). When deposited on a substrate, the stabilized chains demonstrate straight parts whose lengths significantly exceed the theoretical limit for a free stable monatomic carbon chain. The high-resolution transmission electron microscopy (HR TEM) of our samples shows straight linear carbon chains of the lengths that sometimes exceed 5 nm. Most interestingly, at the liquid helium temperature, a pronounced fine structure emerges in the photoluminescence (PL) spectra of the deposited carbon chains on the top of broad resonances corresponding to polyyne chains of different lengths. This fine structure is composed invariably of a high-amplitude narrow peak accompanied by two lower-energy satellites which can be attributed to the exciton resonance and two trion resonances, respectively. The time-resolved photoluminescence (TRPL) spectra show that the radiative lifetime of the observed transitions is of the order of 1 ns, which is similar to the data reported for excitons in carbon nanotubes (CNTs).[19] At high temperatures, the double exponential decay of the PL signal is

https://dx.doi.org/10.1021/acs.nanolett.0c02244
Nano Lett. 2020, 20, 6502−6509

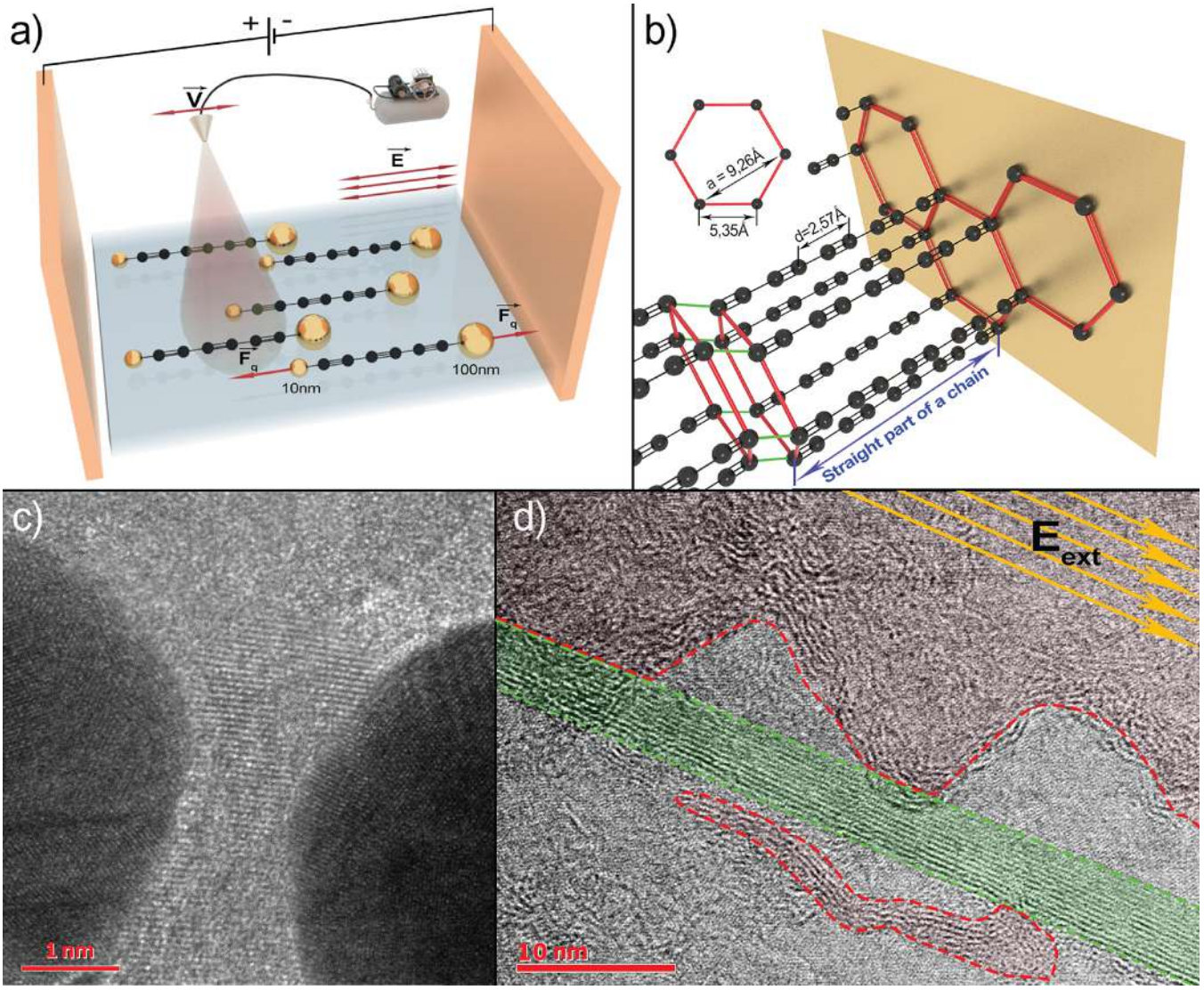

Figure 2. Deposition and characterization of carbon chains: (a) Illustration of our method of deposition of the aligned carbon chains stabilized by gold NPs of different sizes. Due to the difference in work functions of gold nanoparticles attached to the ends of a carbon chain, it becomes dipole polarized. The external electric field orients the polarized chains, so that over a half of them appear to be aligned when deposited on a substrate by sputtering. (b) Schematics of the structure of a quasicrystal formed by polyyne wires attached to a gold NP (shown as a yellow wall) that is based on the X-ray diffraction analysis.[23] (c) HR TEM image of bundles of carbon chains attached to two gold NPs of a nearly spherical shape, seen as the dark regions on the left-hand side and right-hand sides of the image. The observed quasicrystal structure is composed by sp-carbon polyyne chains and represents a van der Waals quasicrystal. Its lattice parameters are a = 0.926 nm and c = 1.25 nm, and the polyyne lattice constant is d = 0.2558 nm. In this case, the distance between neighboring chains in the hexagon is 0.535 nm, in full agreement with the HR TEM image of the central part of the field oriented bundle shown in part d. The green area corresponds to the field-aligned polarized chains end-capped with Au NPs; the red area is occupied by randomly oriented unpolarized chains.

observed with a fast exponential characterizing the thermal dissociation of excitons, and the slow exponential corresponding to their radiative decay. The exciton radiative lifetime decreases with the decrease of the length of the chain. We refer to the Su−Schrieffer−Heeger model[20] to argue that the transition that dominates low-temperature PL spectra is based on the edge electronic states that form the HOMO−LUMO pair in carbon chains stabilized by gold NPs. This interpretation is confirmed by the *ab initio* calculation (Figure 5e−g).

Results. *Synthesis of Monatomic Carbon Chains.* We employed the LAL method for synthesis of the linear carbon chains.[29] The laser processing resulted in the formation of polyyne threads.[24] The stabilization of linear carbon chains is achieved by adding spherical gold NPs to the solution.[21,22] The procedure is schematically illustrated in Figure 1c. NPs having average sizes of either 10 or 100 nm attach themselves to the ends of carbon chains by single electron bonds. As the folding of chains and formation of kinks also occur predominantly at the single bonds, the parity rule is imposed to the number of atoms belonging to straight parts of the chains. Here, in particular, we observe spectral resonances of the straight chains containing even numbers of C atoms ranging from 8 to 24. Typically, these are straight parts of longer linear chains attached by both ends to gold NPs. Kinks separate each linear chain into several straight parts. It is important to note also that if NPs at the opposite ends of a carbon chain are of different sizes, the difference of their work functions results in

https://dx.doi.org/10.1021/acs.nanolett.0c02244
Nano Lett. 2020, 20, 6502−6509

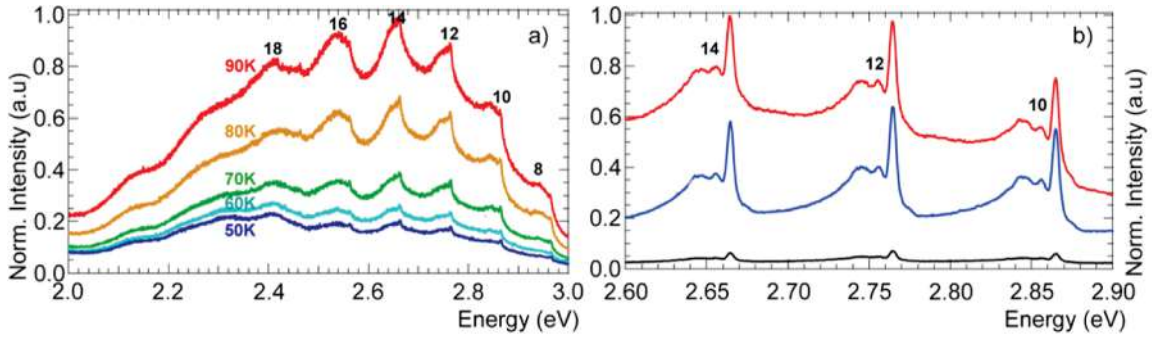

Figure 3. PL spectra of the deposited polyyne chains of different lengths (the number of atoms in the chain is indicated on the top of the corresponding spectral resonance). (a) Spectra taken at temperatures from 90 to 50 K (red curve corresponds to 90 K, yellow curve to 80 K, green curve to 70 K, teal curve to 60 K, and blue curve to 50 K). The laser excitation wavelength is 390 nm with the intensity of 5 mW and the acquisition time of 10 s. (b) PL spectra taken at 4 K. Red, blue, and black curves correspond to the excitation wavelengths of 390, 380, and 370 nm, respectively. The acquisition time is 40 s.

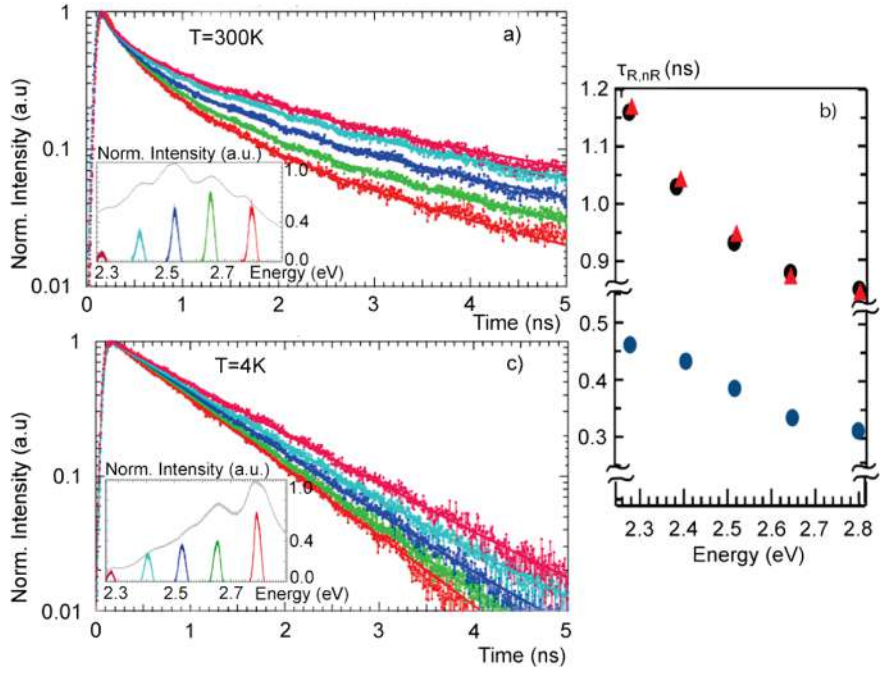

Figure 4. Time-resolved photoluminescence (TRPL) data. (a, c) TRPL signal acquired at the room temperature and at 4 K, respectively. The insets show the spectral bands that correspond to the TRPL curves of parts a and c, respectively. (b) The colors match shows the extracted decay times of the TRPL signal taken at room temperature and helium temperature, respectively. Red and black points correspond to the deduced radiative decay time at the room temperature (red) and helium temperature (black). The blue points show the nonradiative decay times, extracted from the room temperature TRPL curves in part a.

the charging of the carbon−NP complex that acquires a stationary dipole moment. This dipole polarization provides a tool for the chain ordering by an applied voltage.[23]

We intentionally ordered the carbon chains by passing the solution through the stationary electric field in the course of sputtering (see the scheme in Figure 2a[23]). As a result, we were able to deposit long parallel chains of polyyne. Figure 2c shows the HR TEM image of a typical bundle of carbon chains attached by both of its ends to gold NPs. Figure 2d shows the HR TEM image of the central part of the bundle of parallel carbon chains of the length exceeding 40 nm. Gold NPs remained outside the frame of the image in this case. Our previous study showed that the ensemble of carbon chains in a bundle forms a kind of one-dimensional van der Waals crystal, where the distance between neighboring chains exceeds the interatomic distance in a single chain d by a factor of 3.6,[23] approximately (see Figure 2b). We note that only about one-half of carbon bundles have gold NPs of different sizes (10 and 100 nm, typically) at their ends. These bundles are dipole polarized due to the difference of the work function of gold NPs of different sizes. They are aligned by the electric field during the sputtering process. These structures are hosts to positively and negatively charged trions that manifest themselves in the low-temperature PL spectra as we show below. The other half of carbon−metal nanostructures are formed by gold NPs of the same size. They are not polarized and not aligned by the electric field. The carbon chains in these structures mostly host electrically neutral excitons. The carbon chains connecting gold NPs are of approximately the same length, which is why they are able to form hexagonal quasicrystal structures. This is confirmed by the X-ray study presented in ref 23. The kinks, indeed, have different locations

https://dx.doi.org/10.1021/acs.nanolett.0c02244
Nano Lett. 2020, 20, 6502−6509

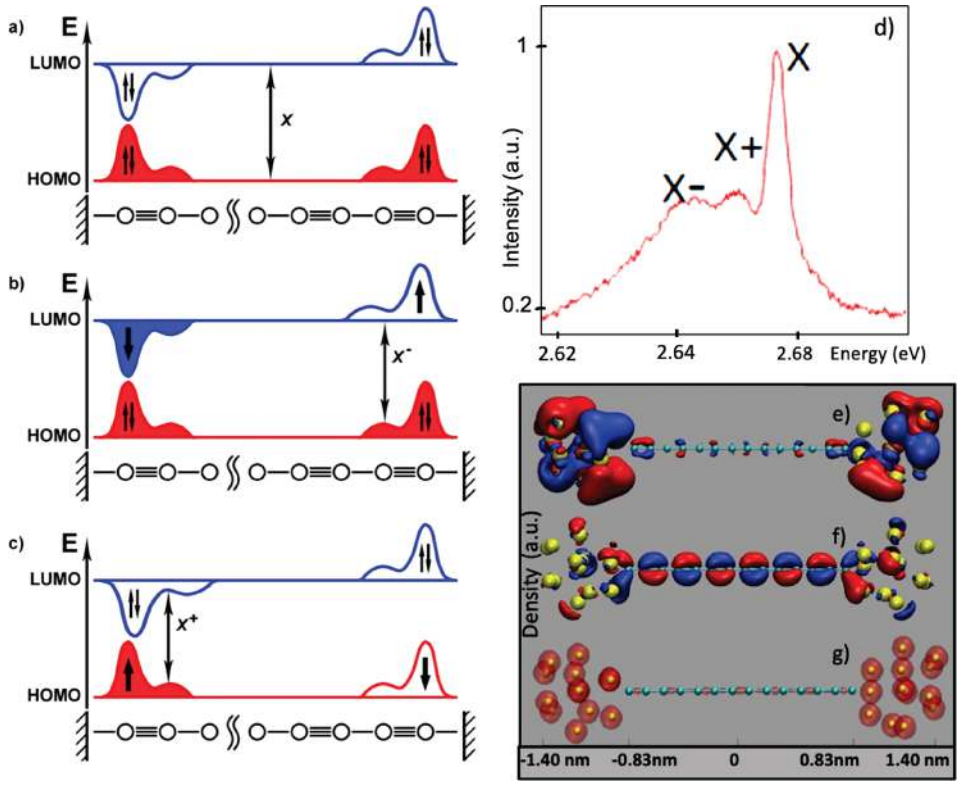

Figure 5. Scheme of excitonic transitions in a finite-size polyyne chain. (a) The neutral exciton (X) is formed by even and odd edge states that originate from the HOMO−LUMO pair. (b, c) Trion transitions in charged chains, where the left−right symmetry is broken so that the optical transition occurs either between the original HOMO state and the spin polarized electron state localized at one of the edges (X−) or between the hole state localized at one of the edges and the original LUMO state (X+). (d) Enlarged PL spectrum of a characteristic triplet corresponding to the 14-atom chain that shows the relative strengths of exciton and trion transitions. Molecular orbitals and total electron density plots for a model system containing a polyyne chain composed of 14 carbon atoms capped with two gold NPs (C14−$Au13_2$) for HOMO (e) and LUMO (f). (g) Total calculated electron density. Red and blue lobes correspond to positive and negative values, respectively.

at different carbon chains. In Figure 2c,d, we show HR TEM images of various carbon bundles typically composed of over 10 parallel chains.

Low-Temperature PL Spectra of the Deposited Polyyne Chains. In the PL experiments, we excited the deposited polyyne chains quasiresonantly, at the wavelengths between 370 and 390 nm. The strong emission at the wavelengths over 400 nm has been detected. As there were necessarily thousands of individual carbon chains under our pump spot, which is of 2 μm size, the PL signal is always built from contributions of carbon chains of different lengths. The chains containing from 8 to 18 atoms[29] typically dominate the spectra. Figure 3a shows the characteristic PL spectra featuring broad resonances corresponding to the chains of different lengths emitting in the spectral range 2.4−3.0 eV. The lowest-energy optical transition shifts to the red with the increase of the length of the chain, in full agreement with the theoretical predictions.[25−29] In Figure 3a we attribute the sequence of spectral resonances observed to the polyyne chains containing from 8 to 22 atoms (the transitions in chains of 8−18 atoms are labeled in the figure) in agreement with the previously reported transition energies[29] and the results of our own *ab initio* calculation. As the temperature goes down to 4 K, a very distinct and peculiar fine structure emerges on the top of each broad PL peak (Figure 3b). Nearly identical triplet structures are observed for the chains of 10, 12, 14, and 16 atoms. A strong and very narrow peak with a full width at half-maximum (fwhm) of only 3−4 meV has two broader and lower satellites shifted by about 15 and 25 meV toward lower energies. This observation is in a stark contrast with the exciton spectra of carbon nanotubes[19] that typically feature strongly inhomogeneously broadened peaks with typical fwhm of several 10s meV. The left panel of Figure 4 shows the time-resolved photoluminescence (TRPL) data acquired at the high temperature (Figure 4a) and liquid helium temperature (Figure 4c). The TRPL is spectrally resolved, the selected bands being indicated in the insets. The high-temperature spectra show the double-exponential behavior reflecting the interplay between nonradiative (presumably, thermal hopping) and radiative channels of the exciton decay. The extracted decay times are plotted in Figure 4b. The low-temperature spectra show the monoexponential decay of the excitonic photoluminescence with a characteristic decay time of the order of 1 ns that is comparable with the typical radiative lifetimes of excitons in carbon nanotubes.[30,31] The exciton radiative lifetime increases with the increase of the length of the chain following the anticipated behavior of the matrix element of the dipole transition. We note that the exciton fine structure observed in CW PL spectra taken at the selective optical excitation cannot be resolved in the TRPL spectra as the pulsed excitation used in this spectroscopy technique is not wavelength selective. Still, the method allows for clearly distinguishing between the nonradiative exciton decay due to the thermal hopping of carriers and the exciton radiative recombination that dominates the low-temperature TRPL dynamics.

https://dx.doi.org/10.1021/acs.nanolett.0c02244
Nano Lett. 2020, 20, 6502−6509

Discussion. The triplet structures emerging as the temperature decreases are indicative of excitonic transitions. It is important to note that the textbook definition of the exciton binding energy as the difference of the transition energy for an electron−hole pair separated by an infinite distance and the exciton optical transition energy cannot be applied in our case, as electron and hole cannot be separated by more than a few nanometers in a van der Waals nanocrystal composed of a handful of carbon chains. The quantity that is relevant to our experimental observations is rather an exciton thermal dissociation energy. It characterizes the difference of the transition energies between an electron and a hole belonging to the same carbon chain and between an electron and a hole located in different (neighboring) carbon chains. The exciton dissociation into a radiatively inactive electron−hole pair by thermal hopping of one of the carriers to the neighboring chains (Figure 2c) is expected to govern the temperature dependence of the intensity of the observed excitonic peaks. From the PL spectra taken at temperatures between 4 and 300 K, we estimate the thermal hopping energy to be of the order of 15−20 meV. This is consistent with our variational calculation performed using the procedure developed in ref 32 for quantum wires. Using the electron and hole effective masses predicted by our *ab initio* calculation as $m_e = 0.078m_0$ and $m_h = 0.09m_0$ with m_0 being a free electron mass, describing both dielectric and metallic screening by an effective dielectric constant eps = 6 for spatially direct and eps = 4 for spatially indirect excitons, we obtain the difference of energies of an exciton formed by an electron and a hole belonging to the same chain and an exciton formed by an electron and a hole belonging to different chains of about 15 meV. Given the strongly limited accuracy of the variational calculation, we find these numbers to be in a very good agreement with the experimental data. Note that the excitons are expected to be localized at the ends of the carbon chains forming an equivalent of Su−Schrieffer−Heeger states[20] as confirmed by the results of our *ab initio* calculation shown in Figure 5e−g.

Two lower-energy satellites clearly visible in the excitonic spectra of the carbon chains containing 10, 12, and 14 atoms may be associated with zero-phonon lines,[33] phonon replicas, biexcitons, or charged excitons, in principle. We rule out the three first scenarios as the following: (i) The measured vibron energies in polyyne are of 130 and 267 meV (Raman spectra are shown in the Supporting Information, Figure S3) that strongly exceed the observed splittings between the main peak and satellite peaks (15−25 meV). (ii) The typical optical phonon energy in polyyne is expected to be of the order of 100 meV[31] that is also significantly larger than the observed splittings. (iii) The biexciton line intensity would vanish at low excitation powers, which contradicts our data. Charged exciton complexes (trions) are likely to be formed in our system due to the vicinity of metal nanoparticles that can supply carbon chains with extra charge carriers (see the schemes in Figure 5b,c and TEM images given in the Supporting Information). The variational calculation predicts the exciton-positively charged trion splitting of about 15 meV and positive−negative trion splitting of 25 meV which is in a good agreement with the data. The strong dipole polarization of approximately a half of gold-stabilized carbon chains is confirmed by their alignment in the external electric field (see the scheme in Figure 3a and the Supporting Information); thus, the presence of extra-charges localized at the ends of some of the chains is beyond any doubt. The spectrally integrated intensities of negatively charged (X−) and positively charged (X+) trion transitions are expected to be lower than the integrated intensity of the neutral exciton transition. Indeed, statistically, having equal concentrations of 10 and 100 nm NPs, one should expect only a half of carbon chains to be attached to the NPs of different radii and hence polarized. In the polarized chains, two of the lowest-energy optical transitions would be either a positively or a negatively charged trion. As every chain is divided into several straight pieces by kinks, neutral excitons can still be formed in central parts of the polarized chains. We conclude that the sum of integrated intensities of X− and X+ lines should be equal to or less that the integrated intensity of the X-line. This is generally consistent with the data (see Figure 5d).

Figure 5e−g presents the plots of HOMO and LUMO wave functions and of the total electron density of Au-stabilized carbon chains, obtained from *in vacuo* DFT calculations with localized basis sets, which are shown for the polyyne chain of 14 carbon atoms capped with two Au13 nanoparticles. Indeed, in the calculated distributions of the HOMO and the total density (top and bottom panel) it appears that most of the electron cloud is located around gold atoms and partially on the shorter C−C bonds of the polyyne moiety. Excitons and trions based on HOMO−LUMO transitions are localized at the ends of the atomic chains. This strong spatial localization and significant electron−hole overlap are responsible for a large oscillator strength of the corresponding optical transitions. The similar plots obtained for C14 without gold terminations (see Figures S6 and S7 of the Supporting Information) lack these features, and the electronic density tends to vanish moving from the center to the ends of the chain. We conclude that gold-stabilized carbon chains are highly advantageous for the observation of excitonic effects as they provide a very strong spatial localization, large oscillator strength, and low inhomogeneous broadening of the exciton and trion transitions.

In conclusion, we show that the sharp peaks emerging at low temperatures in the PL spectra of gold-stabilized carbon chains are indicative of the exciton and trion transitions based on the edge electronic states in the chains. The triplet fine structure that is very well seen at helium temperature is essentially independent of the length of the chain, while the absolute energies of the transitions become larger for the shorter chains. This observation demonstrates a high potentiality of synthesized polyyne chains for optoelectronic applications, especially in nanolasing and single photon emitters. Moreover, the observation of radiatively active excitons in ultimate one-dimensional carbon crystals is of a great fundamental interest. Further studies are needed to fully reveal properties of excitons and trions in carbon chains.

■ ASSOCIATED CONTENT

Supporting Information

The Supporting Information is available free of charge at https://pubs.acs.org/doi/10.1021/acs.nanolett.0c02244.

Detailed description of the synthesis of linear carbon chains in a liquid, experimental method of measurements and orientated deposition, and the *ab initio* calculation details (PDF)

https://dx.doi.org/10.1021/acs.nanolett.0c02244
Nano Lett. 2020, 20, 6502−6509

AUTHOR INFORMATION

Corresponding Author

Stella Kutrovskaya − *School of Science, Westlake University, Hangzhou 310024, China; Institute of Natural Sciences, Westlake Institute for Advanced Study, Hangzhou 310024, China; Department of Physics and Applied Mathematics, Stoletov Vladimir State University, Vladimir 600000, Russia;* orcid.org/0000-0003-4568-3995; Email: stella.kutrovskaya@westlake.edu.cn

Authors

Anton Osipov − *Department of Physics and Applied Mathematics, Stoletov Vladimir State University, Vladimir 600000, Russia; ILIT RAS—Branch of FSRC "Crystallography and Photonics" RAS, Shatura 140700, Russia;* orcid.org/0000-0002-1968-8795

Stepan Baryshev − *Skolkovo Institute of Science and Technology, Moscow 121205, Russia;* orcid.org/0000-0002-6036-9235

Anton Zasedatelev − *Skolkovo Institute of Science and Technology, Moscow 121205, Russia;* orcid.org/0000-0003-0414-5779

Vladislav Samyshkin − *Department of Physics and Applied Mathematics, Stoletov Vladimir State University, Vladimir 600000, Russia;* orcid.org/0000-0002-0636-2374

Sevak Demirchyan − *School of Science, Westlake University, Hangzhou 310024, China; Institute of Natural Sciences, Westlake Institute for Advanced Study, Hangzhou 310024, China;* orcid.org/0000-0002-6330-1367

Olivia Pulci − *Department of Physics, University of Rome Tor Vergata, I-00133 Rome, Italy;* orcid.org/0000-0002-9725-487X

Davide Grassano − *Department of Physics, University of Rome Tor Vergata, I-00133 Rome, Italy;* orcid.org/0000-0001-8821-6452

Lorenzo Gontrani − *Department of Physics, University of Rome Tor Vergata, I-00133 Rome, Italy;* orcid.org/0000-0001-8212-7029

Richard Rudolph Hartmann − *Physics Department, De La Salle University, 0922 Manila, Philippines;* orcid.org/0000-0002-1708-0540

Mikhail E. Portnoi − *Physics and Astronomy, University of Exeter, Exeter EX4 4QL, United Kingdom; ITMO University, St. Petersburg 197101, Russia;* orcid.org/0000-0001-5618-0993

Alexey Kucherik − *Department of Physics and Applied Mathematics, Stoletov Vladimir State University, Vladimir 600000, Russia;* orcid.org/0000-0003-0589-9265

Pavlos G. Lagoudakis − *Skolkovo Institute of Science and Technology, Moscow 121205, Russia;* orcid.org/0000-0002-3557-5299

Alexey Kavokin − *School of Science, Westlake University, Hangzhou 310024, China; Institute of Natural Sciences, Westlake Institute for Advanced Study, Hangzhou 310024, China; Spin Optics Laboratory, St. Petersburg State University, St. Petersburg 198504, Russia;* orcid.org/0000-0003-2713-1062

Complete contact information is available at: https://pubs.acs.org/10.1021/acs.nanolett.0c02244

Notes

The authors declare no competing financial interest.

ACKNOWLEDGMENTS

The work of S.K., S.D., and A.KA. is supported by the Westlake University (Project 041020100118) and by the Program 2018R01002 of Leading Innovative and Entrepreneur Team Introduction Program of Zhejiang. RFBR grants 18-32-20006 and 19-32-90085 sponsored the work of S.K. and V.S.; 20-52-12026 and 20-02-00919 of S.B., A.Z., and P.L.; and the RScF grant 20-72-10145 to A.Z. A.KA. acknowledges Saint-Petersburg State University for the research grant ID 51125686. Funding by the EU MSCA RISE project "DiSeTCom" (GA823728) is gratefully acknowledged by O.P. and TERASSE (GA 823878) by M.E.P. and R.R.H. A.O. acknowledges the Ministry of Science and Higher Education within the State assignment FSRC Crystallography and Photonics RAS (Project 075-00842-20-00). The work of M.E.P. was supported by the ITMO Fellowship and Professorship Program 5-100. L.G. acknowledges support from Regione Lazio, through Progetto di Ricerca 85-2017-15125 according to L. R. 13/08. CPU computing time was granted by CINECA HPC center and by the "Departments of Excellence-2018" Program (Dipartimenti di Eccellenza) of the Italian Ministry of Research, DIBAF-Department of University of Tuscia, Project "Landscape 4.0—food, wellbeing and environment". The synthesis and deposition of LLCC have been performed at the Vladimir State University. Raman spectra and absorbance were measured at the Center for Optical and Laser Materials Research, Research Park, St. Petersburg State University.

REFERENCES

(1) Segawa, Y.; Ito, H.; Itami, K. Structurally uniform and atomically precise carbon nanostructures. *Nature Reviews Materials* **2016**, *1*, 15002.

(2) Goresy, A. E.; Donnay, G. A new allotropic form of carbon from the ries crater. *Science* **1968**, *161*, 363.

(3) Whittaker, A. Carbon: Occurrence of carbyne forms of carbon in natural graphite. *Carbon* **1979**, *17*, 21−24.

(4) Chuan, X.-Y.; Zheng, Z.; Chen, J. Flakes of natural carbyne in a diamond mine. *Carbon* **2003**, *41*, 1877−1880.

(5) Casari, C. S.; Tomassini, M.; Tykwinski, R. R.; Milani, A. Carbon-atom wires: 1-D systems with tunable properties. *Nanoscale* **2016**, *8*, 4414.

(6) Casari, C. S.; Milani, A. Carbyne: from the elusive allotrope to stable carbon atom wires. *MRS Commun.* **2018**, *8*, 207.

(7) Kroto, H. Carbyne and other myths about carbon. *Chemistry World* **2010**, *7*.

(8) Landau, L.; Lifshitz, E. *Statistical physics, part 1 (course of theoretical physics*; Butterworth-Heinemann, 1980; Vol. *5*.

(9) Gibtner, T.; Hampel, F.; Gisselbrecht, J.-P.; Hirsch, A. End-cap stabilized oligoynes: Model compounds for the linear sp carbon allotrope carbyne. *Chem. - Eur. J.* **2002**, *8*, 408−432.

(10) Casillas, G.; Mayoral, A.; Liu, M.; Ponce, A.; Artyukhov, V. I.; Yakobson, B. I.; Jose-Yacaman, M. New insights into the properties and interactions of carbon chains as revealed by HR-TEM and DFT analysis. *Carbon* **2014**, *66*, 436.

(11) Shi, L.; Rohringer, P.; Suenaga, K.; Niimi, Y.; Kotakoski, J.; Meyer, J. C.; Peterlik, H.; Wanko, M.; Cahangirov, S.; Rubio, A.; Lapin, Z.; Novotny, L.; Ayala, P.; Pichler, T. Conned linear carbon chains as a route to bulk carbyne. *Nat. Mater.* **2016**, *15*, 634−639.

(12) Rabia, A.; Tumino, F.; Milani, A.; Russo, V.; Li Bassi, A.; Achilli, S.; Fratesi, G.; Onida, G.; Manini, N.; Sun, Q.; Hu, W.; Casari, C. S. Scanning tunneling microscopy and Raman spectroscopy of polymeric sp-sp2 carbon atomic wires synthesized on the Au(111) surface. *Nanoscale* **2019**, *11*, 18191.

(13) Chalifoux, W. A.; Tykwinski, R. R. Synthesis of polyynes to model the sp-carbon allotrope carbyne. *Nat. Chem.* **2010**, *2*, 967.

(14) Khanna, R.; Ikram-Ul-Haq, M.; Rawal, A.; Rajarao, R.; Sahajwalla, V.; Cayumil, R.; Mukherjee, P. S. Formation of carbyne-like materials during low temperature pyrolysis of lignocellulosic biomass: A natural resource of linear sp carbons. *Sci. Rep.* **2017**, *7*, 16832.
(15) Liu, M.; Artyukhov, V. I.; Lee, H.; Xu, F.; Yakobson, B. I. Carbyne from first-principles: Chain of C atoms, a nanorod or a nanorope. *ACS Nano* **2013**, *7*, 10075.
(16) Itzhaki, L.; Altus, E.; Basch, H.; Hoz, S. Harder than diamond: Determining the crosssectional area and Youngs modulus of molecular rods. *Angew. Chem., Int. Ed.* **2005**, *44*, 7432−7435.
(17) Ma, C. R.; Xiao, J.; Yang, G. W. Giant nonlinear optical responses of carbyne. *J. Mater. Chem. C* **2016**, *4*, 4692.
(18) Xiao, J.; Li, J.; Yang, G. Molecular luninescence of white carbon. *Small* **2017**, *13*, 1603495.
(19) Shaver, J.; Kono, J. Temperature-dependent magneto-photoluminescence spectroscopy of carbon nanotubes: evidence for dark excitons. *Laser and Photon. Rev.* **2007**, *1* (3), 260.
(20) Su, W. P.; Schrieffer, J. R.; Heeger, A. J. Solitons in polyacetylene. *Phys. Rev. Lett.* **1979**, *42*, 1698.
(21) Kucherik, A. O.; Arakelian, S. M.; Garnov, S. V.; Kutrovskaya, S. V.; Nogtev, D. S.; Osipov, A. V.; Khor'kov, K. S. Two-stage laser-induced synthesis of linear carbon chains. *Quantum Electron.* **2016**, *46*, 627.
(22) Yazyev, O. V.; Pasquarello, A. Effect of metal elements in catalytic growth of carbon nanotubes. *Phys. Rev. Lett.* **2008**, *100*, 156102.
(23) Kutrovskaya, S.; Chestnov, I.; Osipov, A.; Samyshkin, V.; Sapegina, I.; Kavokin, A.; Kucherik, A. Electric field assisted alignment of monoatomic carbon chains. *Sci. Rep.* **2020**, *10*, 9709.
(24) Kucherik, A.; Arakelian, S.; Vartanyan, T.; Kutrovskaya, S.; Osipov, A.; Povolotskaya, A.; Povolotskii, A.; Man'shina, A. Laser-induced synthesis of metalcarbon materials for implementing surface-enhanced Raman scattering. *Opt. Spectrosc.* **2016**, *121*, 263−270.
(25) Heimann, R. B.; Evsyukov, S. E.; Kavan, L. *Carbyne and carbynoid structures*; Springer Science & Business Media, 1999; Vol. *21*.
(26) Cataldo, F. Synthesis of polyynes in a submerged electric arc in organic solvents. *Carbon* **2004**, *42*, 129−142.
(27) Peierls, R. Transition temperatures. *Helvetica Physica Acta* **1934**, *2*, 7.
(28) Buntov, E. A.; Zatsepin, A. F.; Guseva, M. B.; Ponosov, Y. S. 2d-ordered kinked carbyne chains: Dft modeling and raman characterization. *Carbon* **2017**, *117*, 271−278.
(29) Pan, B.; Xiao, J.; Li, J.; Liu, P.; Wang, C.; Yang, G. Carbyne with finite length: The one-dimensional sp carbon. *Science Advances* **2015**, *1*, e1500857.
(30) Amori, A. R.; Hou, Zh.; Krauss, T. D. Excitons in Single-Walled Carbon Nanotubes and Their Dynamic. *Annu. Rev. Phys. Chem.* **2018**, *69*, 81.
(31) Mostaani, E. Quasiparticles and excitonic gaps of one-dimensional carbon Chains. *Phys. Chem. Chem. Phys.* **2016**, *18*, 14810.
(32) Kavokin, A.V.; Baumberg, J.J.; Malpuech, G.; Laussy, F.P. *Microcavities*, 2nd ed.; Oxford University Press, 2017; Chapter 4, section 4.3.4.
(33) Tamarat, P.; Maali, A.; Lounis, B.; Orrit, M. Probing the spectral dynamics of single terrylenediimide molecules in low-temperature solids. *J. Phys. Chem. A* **2000**, *104*, 1.

https://dx.doi.org/10.1021/acs.nanolett.0c02244
Nano Lett. 2020, 20, 6502−6509